**Preprints of the 19th World Congress**
**The International Federation of Automatic Control**
**Cape Town, South Africa. August 24-29, 2014**

# Plant-wide control of a parabolic trough power plant with thermal energy storage ⋆

**Michael Jost** *, **Wolfgang Grote** **, **Florian Möllenbruck** *, **Martin Mönnigmann** *

* *Automatic Control and Systems Theory, Ruhr-Universität Bochum, Bochum, Germany*
** *MAN Diesel & Turbo SE, Oberhausen, Germany*

**Abstract:** We present a control scheme for a parabolic trough power plant that is equipped with a molten salt thermal energy storage system. We show that the multivariable control problem for the solar field can be decoupled by controlling the three way valve that splits the heat transfer fluid between the storage system and the steam generator. The steam generation cycle is regulated with inlet pressure control. The subsystems of the plant are modeled based on first principles, where we focus on the steam generation cycle. A multi-group extraction turbine with pre- and reheater is considered, which is suitable for solar power plants. We demonstrate the benefits of the proposed control scheme with a day-to-day simulation.

*Keywords:* Control of power plants, solar power plants, thermal energy storage, decoupling control

Technology for solar energy based power generation belongs to one of two categories: direct usage, most prominently implemented in photovoltaic cells, and indirect usage that is based on concentrating devices, such as parabolic trough systems (Camacho et al., 2010). The latter reflect solar irradiation onto an absorber pipe, which runs in the focal line of a reflector mirror. Solar energy is absorbed by a heat transfer fluid (HTF) that flows inside the absorber pipe. Finally, the collected thermal energy is delivered to a steam turbine, which drives a generator. One drawback of these solar power plants is that the main power source, the sun, cannot be controlled. Obviously, this restricts the operation time of solar power plants. Modern plants are equipped with thermal storage systems that mitigate fluctuations and that are used to extend the operating hours beyond daylight time. This makes solar power plants much more attractive, but increases their complexity from a control point of view.

In this paper we deal with the plant-wide control of a solar power plant equipped with a molten salt thermal storage system. Various controllers have been developed for solar power plants, such as fuzzy controllers, model predictive controllers or internal mode controllers, to name just a few. We refer to the survey papers (Camacho et al., 2007a,b) and references therein.

If the solar irradiation is insufficient to run the plant at its nominal power level, the storage system is used as an auxiliary energy source. We show how the solar part of the plant can be controlled in this situation. We consider the three way valve that splits the HTF mass flow between the storage system and the steam generator to be an additional control input. The HTF flow rate is kept constant in this setup. This decouples the solar part of the plant into two subsystems, which can be controlled separately. Surplus energy collected at daytime can be used to charge the storage tanks with a similar control concept based on a second three way valve. The power generation block of the power plant is regulated with inlet pressure control.

We derive mathematical models for each subsystem of the solar power plant in Sec. 1. Section 2 details the control approach. Results are presented in Section 3. The paper closes with brief conclusions in Sec. 4.

## 1. PLANT MODEL

The solar power plant considered here is equipped with a molten salt thermal storage tank (Pacheco et al., 2001). Figure 1 shows a schematic sketch of the plant, which is designed for 50MW electrical power at nominal operation. The steam generator is driven by the HTF flow rate $\dot{q}_{\mathrm{f},3}$ with inlet temperature $T_{\mathrm{f},3}$. The remainder of the plant is a conventional combination of steam turbine and generator. We use a Rankine cycle to model the generation of mechanical power. The steam turbine is modeled as a multi-group turbine with reheater and preheater. A condenser closes the thermodynamic cycle. We summarize the differential equations for each of these subsystems in the remainder of this section.

### 1.1 Notation

We denote by $\dot{m}$, $\dot{q}$, $T$, $\rho$, $c$, $A$ the mass flow rate, volume flow rate, temperature, density, specific heat capacity and cross-sectional area, respectively. Indices m, f, s and w are used to refer to the pipe metal, the HTF, the molten salt and the water/steam, respectively. Indices Dis and Chg

⋆ Support by the European Union under the European Regional Development Fund is gratefully acknowledged.

EUROPEAN UNION Investing in our Future European Regional Development Fund
Ziel2.NRW Regionale Wettbewerbsfähigkeit und Beschäftigung
Ministerium für Innovation, Wissenschaft und Forschung des Landes Nordrhein-Westfalen

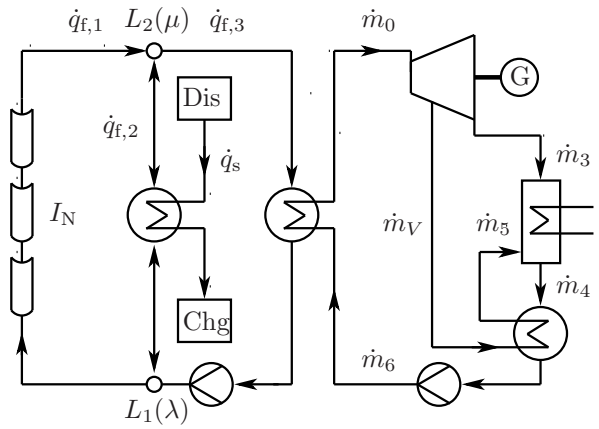


Fig. 1. Schematic sketch of the solar power plant. HTF (flow rate $\dot{q}_{\mathrm{f},1}$) is heated in the collector field by solar irradiation $I_{\mathrm{N}}$. A molten salt storage system can be used as second energy source (HTF flow rate $\dot{q}_{\mathrm{f},2}$). The steam turbine is modeled as a two group extraction turbine, where the mass flow rate $\dot{m}_{\mathrm{V}}$ is extracted after the first turbine group and used to preheat feedwater.

refer to the discharging and charging mode of the heat storage, respectively.

### *1.2 Physical models of the subsystems*

Thermal properties of the thermal fluid, the molten salt and water and steam are assumed to be temperature dependent. See App. A for a brief summary.

*Collector field:* According to Powell and Edgar (2011) and Camacho et al. (2007a, 1997), the collector field can be described by the partial differential equations

$$\begin{aligned}\rho_{\mathrm{m}} c_{\mathrm{m}} A_{\mathrm{m}} \frac{\partial T_{\mathrm{m}}}{\partial t} &= \eta_0 D I_{\mathrm{N}} - G H_{\mathrm{l}}(T_{\mathrm{m}} - T_{\mathrm{a}}) - L H_{\mathrm{t}}(T_{\mathrm{m}} - T_{\mathrm{f}}),\\ \rho_{\mathrm{f}} c_{\mathrm{f}} A_{\mathrm{f}} \frac{\partial T_{\mathrm{f}}}{\partial t} + \rho_{\mathrm{f}} c_{\mathrm{f}} \dot{q}_{\mathrm{f}} \frac{\partial T_{\mathrm{f}}}{\partial x} &= L H_{\mathrm{t}}(T_{\mathrm{m}} - T_{\mathrm{f}}),\end{aligned} \tag{1}$$

where $I_{\mathrm{N}}$ denotes the solar irradiation, $D$ is the mirror width, $G$ is the inner diameter of the pipe, $L$ is the outer diameter of the pipe, $\eta_0$ is the efficiency, $T_{\mathrm{a}}$ is the ambient temperature and $H_{\mathrm{l}}(T_{\mathrm{m}})$ and $H_{\mathrm{t}}(\dot{q}_{\mathrm{f}}, T_{\mathrm{f}})$ are the heat exchange coefficients. Note that these coefficients are not constant but depend on the current pipe and fluid temperatures $T_{\mathrm{m}}$, $T_{\mathrm{f}}$, respectively. We adopt these coefficients from (Camacho et al., 1997, p. 29 ff.). We discretize (1) using $\frac{\partial T_{\mathrm{f}}(t,x)}{\partial x} \approx \frac{T_{\mathrm{f}}(x,t) - T_{\mathrm{f}}(x-\Delta x,t)}{\Delta x}$ for small $\Delta x$. Setting $T_{\mathrm{f}}(x,t) = T_{\mathrm{f},i}$ and $T_{\mathrm{f}}(x-\Delta x,t) = T_{\mathrm{f},i-1}$, this yields

$$\begin{aligned}\rho_{\mathrm{m}} c_{\mathrm{m}} A_{\mathrm{m}} \dot{T}_{\mathrm{m},i} &= \eta_0 D I_{\mathrm{N}} - G H_{\mathrm{l}}(T_{\mathrm{m},i} - T_{\mathrm{a}}) - L H_{\mathrm{t}}(T_{\mathrm{m},i} - T_{\mathrm{f},i}),\\ \rho_{\mathrm{f}} c_{\mathrm{f}} A_{\mathrm{f}} \dot{T}_{\mathrm{f},i} + \rho_{\mathrm{f}} c_{\mathrm{f}} \dot{q}_{\mathrm{f}} \frac{T_{\mathrm{f},i} - T_{\mathrm{f},i-1}}{\Delta x} &= L H_{\mathrm{t}}(T_{\mathrm{m},i} - T_{\mathrm{f},i}),\end{aligned} \tag{2}$$

where we assume that the same solar irradiation $I_{\mathrm{N}}$ applies to all mirrors. The collector field considered here contains 312 rows of absorber pipes of 250m length each. We discretize each row into 10 elements ($i = 1, \ldots, 10$ in (2)) with 25m length each.

*Molten salt storage tanks:* Charging and discharging are described with separate models. Both models are based on energy and mass balances, where we assume adiabatic behavior. Assuming that no fluid enters the tank labeled Dis in Fig. 1 during discharging, the model reads

$$\dot{m}_{\mathrm{s,Dis}} = -\rho_{\mathrm{s}} \dot{q}_{\mathrm{s}}, \quad \dot{T}_{\mathrm{s,Dis}} = 0,$$

where $\dot{q}_{\mathrm{s}}$ is the discharging flow rate. Assuming no fluid leaves the storage tank labeled Chg in Fig. 1 during charging, the model is given by

$$\begin{aligned}\dot{m}_{\mathrm{s,Chg}} &= \rho_{\mathrm{s}} \dot{q}_{\mathrm{s}},\\ \dot{T}_{\mathrm{s,Chg}} &= \frac{\dot{q}_{\mathrm{s}}}{c_{\mathrm{s,Chg}} m_{\mathrm{s,Chg}}} \left( c_{\mathrm{s}} T_{\mathrm{s}} \rho_{\mathrm{s}} - \rho_{\mathrm{s,Chg}} c_{\mathrm{s,Chg}} T_{\mathrm{s,Chg}} \right),\end{aligned}$$

where $\dot{q}_{\mathrm{s}}$ is the molten salt flow rate entering the tank and $T_{\mathrm{s}}$ is its temperature.

*HTF to molten salt heat exchanger:* We assume a countercurrent heat exchanger is used to transAfer heat between the molten salt and the HTF. Applying the first law of thermodynamics to this subsystem leads to the differential equations for the temperatures $T_{\mathrm{f,2,b}}$, $T_{\mathrm{s,b}}$ of the HTF and the molten salt, respectively, which read

$$\dot{T}_{\mathrm{f,2,b}} = k_{\mathrm{f,a}} \dot{q}_{\mathrm{f},2} T_{\mathrm{f,2,a}} - k_{\mathrm{f,b}} \dot{q}_{\mathrm{f},2} T_{\mathrm{f,2,b}} - k_{\Delta T} \Delta\vartheta_{\log}(\Delta T_{\mathrm{A}}, \Delta T_{\mathrm{B}}), \tag{3}$$

$$\dot{T}_{\mathrm{s,b}} = k_{\mathrm{s,a}} \dot{q}_{\mathrm{s}} T_{\mathrm{s,a}} - k_{\mathrm{s,b}} \dot{q}_{\mathrm{s}} T_{\mathrm{s,b}} + k_{\Delta T} \Delta\vartheta_{\log}(\Delta T_{\mathrm{A}}, \Delta T_{\mathrm{B}}), \tag{4}$$

where $k_{\mathrm{f,a}}$, $k_{\mathrm{f,b}}$, $k_{\mathrm{s,a}}$ and $k_{\mathrm{s,b}}$ are temperature-dependent coefficients that model the thermal properties of the fluids, $k_{\Delta T} = kA$ is a heat transfer coefficient, and indices a and b refer to inlets and outlets, respectively. The logarithmic temperature difference $\Delta\vartheta_{\log}(\Delta T_{\mathrm{A}}, \Delta T_{\mathrm{B}})$ (Incropera et al., 2007, p. 670 ff.) is defined by

$$\Delta\vartheta_{\log}(\Delta T_{\mathrm{A}}, \Delta T_{\mathrm{B}}) = \begin{cases} \dfrac{\Delta T_{\mathrm{A}} - \Delta T_{\mathrm{B}}}{\ln(\Delta T_{\mathrm{A}}) - \ln(\Delta T_{\mathrm{B}})}, & \Delta T_{\mathrm{A}} \Delta T_{\mathrm{B}} > 0,\\ 0, & \text{else}, \end{cases} \tag{5}$$

where $\Delta T_{\mathrm{A}} = T_{\mathrm{f,2,a}} - T_{\mathrm{s,b}}$ and $\Delta T_{\mathrm{B}} = T_{\mathrm{f,2,b}} - T_{\mathrm{s,a}}$.

*Mixers:* Assume two fluids with mass flows $\dot{m}_{\mathrm{f},1}$, $\dot{m}_{\mathrm{f},2}$, specific heat capacities $c_{\mathrm{f},1}$, $c_{\mathrm{f},2}$ and temperatures $T_{\mathrm{f},1}$, $T_{\mathrm{f},2}$, respectively, are mixed. Then the mass flow $\dot{m}_{\mathrm{f}} = \dot{m}_{\mathrm{f},1} + \dot{m}_{\mathrm{f},2}$ and temperature

$$T_{\mathrm{f}} = \frac{\dot{m}_{\mathrm{f},1} c_{\mathrm{f},1} T_{\mathrm{f},1} + \dot{m}_{\mathrm{f},2} c_{\mathrm{f},2} T_{\mathrm{f},2}}{\dot{m}_{\mathrm{f},1} c_{\mathrm{f},1} + \dot{m}_{\mathrm{f},2} c_{\mathrm{f},2}}.$$

result at the outlet of the mixer.

*Valves:* Consider the three way valve $L_1(\lambda)$ with inlet mass flow and temperature $\dot{m}_{\mathrm{f}}$ and $T_{\mathrm{f}}$, respectively, which splits the HTF flow rate into $\dot{m}_{\mathrm{f},1}$ and $\dot{m}_{\mathrm{f},2}$. Let $\lambda \in [0, ..., 1]$ be the valve parameter. Then the outlet mass flows are given by

$$\dot{m}_{\mathrm{f},1} = \lambda \dot{m}_{\mathrm{f}}, \qquad \dot{m}_{\mathrm{f},2} = (1-\lambda) \dot{m}_{\mathrm{f}}.$$

We assume the thermal properties of the fluids do not change across the valve, which yields $T_{\mathrm{f},1} = T_{\mathrm{f}}$, $T_{\mathrm{f},2} = T_{\mathrm{f}}$.

*Steam generator:* The steam generator model consists of three subsystems: A preheater is used to heat the liquid water to the saturated liquid line, then an evaporator is used to model the change of the enthalpy in the wet steam region and finally, a superheater is used to model the enthalpy change in the generated steam.

Both the preheater and superheater are modeled as counterflow heat exchangers. We only summarize the results for the preheater. The energy balance of this subsystem leads to the differential equation

$$\dot{T}_{\mathrm{f},7} = \frac{\dot{m}_{\mathrm{f},7}}{m_{\mathrm{f},7}} (T_{\mathrm{f},6} - T_{\mathrm{f},7}) - \frac{kA}{m_{\mathrm{f},7} c_{\mathrm{f}}} \Delta\vartheta_{\log}(T_{\mathrm{f},7} - T_{\mathrm{w},6}, T_{\mathrm{f},6} - T_{\mathrm{w},7}),$$

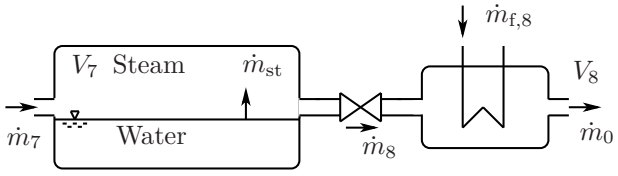


Fig. 2. Model of the steam generation process considered in this paper. The feedwater is vaporized in the evaporator (left), and the generated steam is overheated in the superheater (right). Since no phase transition takes place in the preheater, this part is not shown here.

where $k$ is the heat transfer coefficient and $\Delta\vartheta_{\log}(T_{\mathrm{f},7} - T_{\mathrm{w},6}, T_{\mathrm{f},6} - T_{\mathrm{w},7})$ is the logarithmic temperature difference (5). A similar differential equation for the HTF temperature in the evaporator can be derived. It reads

$$\dot{T}_{\mathrm{f},8} = \frac{2\dot{m}_{\mathrm{f},8}}{m_{\mathrm{f},8}}(T_{\mathrm{f},7} - T_{\mathrm{f},8}) - \frac{2kA}{m_{\mathrm{f},8}c_{\mathrm{f}}}\Delta\vartheta_{\log}(T_{\mathrm{f},8} - T_{\mathrm{w},7}, T_{\mathrm{f},7} - T_{\mathrm{w},8}),$$

where we have assumed that only 50% of the coils are immersed in feedwater.

We describe the pressure and steam generation in the steam generator next; see Fig. 2 for its layout. The pressure generation in both subsystems is modeled with a finite volume approximation. This yields

$$\dot{p}_7 = \frac{\kappa R T_7 z}{V_7}(\dot{m}_{\mathrm{st}} - \dot{m}_8),$$
$$\dot{p}_8 = \frac{\kappa R T_8 z}{V_8}(\dot{m}_8 - \dot{m}_0),$$

where $\kappa$ is the isentropic exponent, $z$ the compressibility factor, $R$ the specific gas constant and $V_i$ and $p_i$ are the corresponding volumina and pressures, respectively, and $T_i$ are the temperatures (Grote, 2009, p. 58).

A throttle valve is used to control the mass flow $\dot{m}_8$ from the steam generator to the boiler. The throttle is modeled as a fluidic resistance with a turbulent flow. According to the Moody diagram (Incropera et al., 2007, p. 491) this yields

$$\dot{m}_8 = \left(\frac{p_7 - p_8}{R}\right)^{\frac{4}{7}}.$$

The enthalpy change of the feedwater and the steam in the steam generator are calculated with the IAPWS-IF97 formulas (Wagner and Kretzschmar, 1997). The total change of enthalpy is given by

$$\Delta h = \Delta h_{\mathrm{P}} + \Delta h_{\mathrm{E}} + \Delta h_{\mathrm{S}},$$

where $\Delta h_{\mathrm{P}} = h'(p_6) - h(p_6, T_6)$ is the enthalpy change in the preheater, $\Delta h_{\mathrm{E}} = h''(p_6) - h'(p_6)$ is the enthalpy change in the evaporator and $\Delta h_{\mathrm{S}} = c\Delta T$ is the enthalpy change in the superheater. Finally, the vaporized fraction of the feedwater $\dot{m}_{\mathrm{st}}$ is given by

$$\dot{m}_{\mathrm{st}} = \frac{kA}{h_{\mathrm{E}}}\Delta\vartheta_{\log}(T_{\mathrm{f},7} - T_{\mathrm{w},6}, T_{\mathrm{f},6} - T_{\mathrm{w},7}),$$

where $h_{\mathrm{E}}$ is the enthalpy of the vaporized water (Sonntag and Van Wylen, 1971, p. 140 ff.).

*Steam turbine:* The steam turbine is modeled as a two group extraction turbine with pre- and reheater. A sketch of the turbine is given in Fig. 3. After the steam has passed the high pressure group, the mass flow rate $\dot{m}_{\mathrm{V}}$ is extracted and used to preheat the feedwater. The remaining mass flow rate $\dot{m}_3$ is reheated using a reheater and fed into the low pressure group. The mass flow entering the high pressure group can be controlled with a valve with characteristics

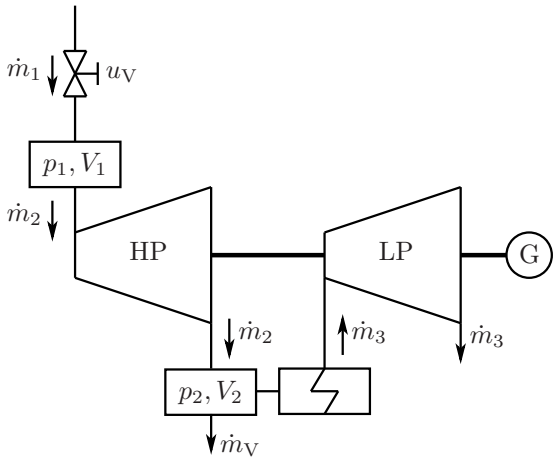


Fig. 3. Simplified schematic representation of the turbine: After passing the high pressure group a fraction of the steam (flow rate $\dot{m}_{\mathrm{V}}$) is used to reheat the feedwater. The remainder (flow rate $\dot{m}_3$) is reheated and fed into the low pressure group.

$$\dot{m}_1 = \dot{m}_0\sqrt{\frac{p_0 T_{0,0}}{T_0 p_{0,0}}}(3u_{\mathrm{V}}^2 - 2u_{\mathrm{V}}^3),$$

where $T_{0,0}$ and $p_{0,0}$ are the operation point temperature and pressure, respectively (Grote, 2009, p. 78 ff.). Note that the normalized valve position is bounded by $0 \leq u_{\mathrm{V}} \leq 1$. The mass flow through the high pressure turbine group can be found using Stodola's law of the ellipse, which yields

$$\dot{m}_2 = K_{\mathrm{ST}}\sqrt{\frac{p_1^2 - p_2^2}{T_1}}, \tag{6}$$

where $K_{\mathrm{ST}}$ is a constant. $K_{\mathrm{ST}}$ is only depends on the nominal turbine design parameters $p_{1,0}$, $p_{2,0}$ and $T_{1,0}$ (Grote, 2009, p. 45 ff.). It is given by

$$K_{\mathrm{ST}} = \dot{m}_0\sqrt{\frac{T_{1,0}}{p_{1,0}^2 - p_{2,0}^2}}. \tag{7}$$

Since the model of the low pressure turbine group is identical to (6) and (7), the equations are not repeated here. Finally, the dynamics of the pressure after the high pressure group are modeled with a finite volume approximation (Grote, 2009, p. 58 ff.), which yields the differential equation

$$\dot{p}_2 = \frac{\kappa R T_2 z}{V_2}(\dot{m}_2 - \dot{m}_{\mathrm{V}} - \dot{m}_3).$$

The pressure dynamics after the low pressure group are included in the condenser. For simplicity, the dynamics of the pipes are neglected.

*Generator:* We model the electrical generator as a synchronous machine, which is coupled to an electric grid. The resulting second order nonlinear differential equation reads

$$\ddot{\varphi} = \frac{1}{\theta}(M_\mathrm{I} - M_\mathrm{T}\sin(\varphi) - d_\mathrm{e}\dot{\varphi}),$$

where $\varphi$ is the rotor angle, $d_\mathrm{e}$ is a damping constant, $M_\mathrm{T}$ is the tilting torque of the machine and $\theta$ is the inertia torque. The power fed into the electrical grid is given by

$$P_\mathrm{e} = M_\mathrm{T}\sin(\varphi)2\pi f_0,$$

where $f_0$ is the nominal grid frequency (Chapman, 2012).

*Preheater and reheater:* The preheater and reheater are modeled as counter flow heat exchangers. Thermal properties of water and steam at the output port are calculated with the IAPWS-IF97 tables (Wagner and Kretzschmar, 1997). The preheater model has to take the phase transition of the extracted steam $\dot{m}_\mathrm{V}$ into account. Since they are analogous to those of the steam generator, the equations are not repeated here.

*Condenser:* Finally, after the steam passes through the low pressure group of the turbine, it is condensed in a condenser, which closes the thermodynamic cycle. The exhaust steam pressure dynamics are modeled with a finite volume again, which yields

$$\dot{p}_4 = \frac{\kappa R T_4 z}{V_\mathrm{C}}(\dot{m}_3 + \dot{m}_5 - \dot{m}_4).$$

Note that this volume is assumed to include the pressure dynamics after the low pressure turbine group. The exhaust steam temperature can be calculated with Magnus's formula

$$T_4 = \frac{c_2 \ln\left(\frac{p_4}{c_0}\right)}{c_1 - \ln\left(\frac{p_4}{c_0}\right)} + 273.15,$$

where $c_0$, $c_1$ and $c_2$ are specific constants (Alduchov and Eskridge, 1996). The dynamics of the cooling water simply follow from the first law of thermodynamics and read

$$\dot{T}_{w,2} = \frac{2\dot{m}_w}{m_w}(T_{w,1} - T_{w,2}) - \frac{2kA}{m_w c_w}\Delta\vartheta_{\log}(T_{w,2} - T_{c,1}, T_{w,1} - T_{c,2}).$$

We assume that the cooling water level is controlled, and 50% of the coils are immersed in water.

*Feedwater pump:* The feedwater pump is modeled as a centrifugal pump. According to Gülich (2010),

$$\Delta p = d_0 + d_1\dot{q} + d_2\dot{q}^2,$$

holds where $d_0$, $d_1$ and $d_2$ are constants and $\Delta p$ is the pressure difference between the inlet and outlet. The latter equation can be extended to include the pump speed, which yields

$$\Delta p = \left(\frac{n}{n_0}\right)^2 d_0 + \left(\frac{n}{n_0}\right) d_1\dot{q} + d_2\dot{q}^2,$$

where $n_0$ denotes the nominal rotary speed, and $n$ is the pump speed (Leonow and Mönnigmann, 2013).

## 2. CONTROLLER DESIGN

Nominal operation corresponds to a HTF flow rate $\dot{q}_{\mathrm{f},3,\mathrm{nom}} = 1.25\frac{\mathrm{m}^3}{s}$ at a temperature $T_{\mathrm{f},3,\mathrm{nom}} = 674\mathrm{K}$. Flow rate and the temperature must be constant during the entire day to maintain the nominal power output. Different controllers are required at night and during sunrise and sunset on the one hand, and during the day on the other hand to achieve nominal operation. Both setups are described in Sec. 2.1. We present the controller design for the steam generation cycle in Sec. 2.2.

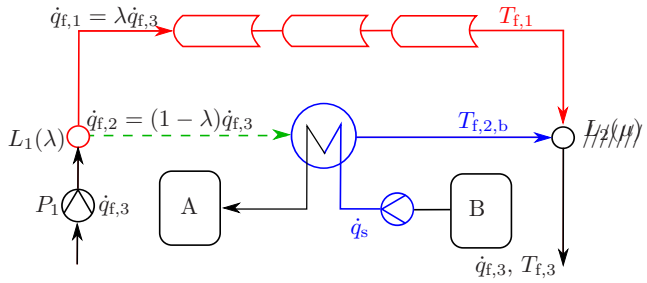


(a) Controller layout during night and sunset/sunrise

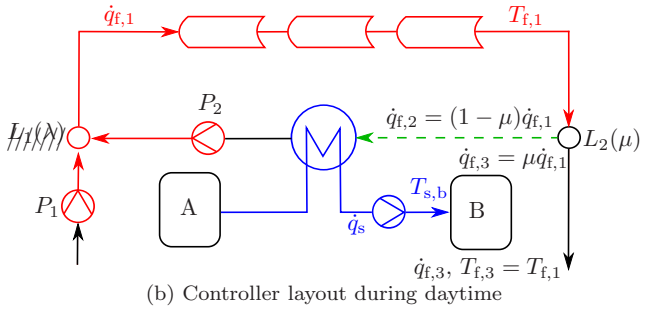


(b) Controller layout during daytime

Fig. 4. Control of the collector field (collector field outlet temperature control loop in red; heat exchanger control loop in blue; known disturbance, which is compensated in the controller, in green). (a) Stored energy is used to drive the plant at night and during sunset/sunrise. If both $T_{\mathrm{f},1}$ and $T_{\mathrm{f},2,\mathrm{b}}$ are at steady state, the temperature of the HTF at the steam generator is constant, too. (b) Collected heat is partially used to run the plant and partially stored for use at night/sunset/sunrise.

### 2.1 Collector field

*Operation at night/sunrise/sunset:* Since the energy collected by the field is insufficient to run the power plant at its nominal power output, the molten salt thermal storage system has to be used as an additional energy source. We use the control layout shown in Fig. 4(a). Essentially, the pump $P_1$ is used to regulate $\dot{q}_{\mathrm{f},3}$ to the constant value $\dot{q}_{\mathrm{f},3,\mathrm{nom}}$, the temperature $T_{\mathrm{f},2,b}$ is regulated to a nominal value with $\dot{q}_\mathrm{s}$, and constant $T_{\mathrm{f},3}$ is achieved by controlling the fraction of the HTF that passes the collector field with the three way valve $L_1(\lambda)$. We explain below that this layout is favorable, because it decouples the control of $\dot{q}_{\mathrm{f},3}$, $T_{\mathrm{f},1}$ and $T_{\mathrm{f},2,b}$. We omit the description of the flow rate controller for $P_1$ and $\dot{q}_{\mathrm{f},3}$ for brevity and discuss the remaining two controllers.

The system of ODEs (2), which describes the collector field and results from discretizing the partial differential equation (1), is nonlinear. Linearization results in a high order transfer function, which can be reduced to the second order transfer function

$$G_\mathrm{f} = \frac{T_{\mathrm{f},1}}{\dot{q}_{\mathrm{f},1}} = \frac{-1.26s - 80.63}{s^2 + 34.4s + 0.42}\cdot 10^{-2}.$$

Since $\dot{q}_{\mathrm{f},1} = \lambda\dot{q}_{\mathrm{f},3,\mathrm{nom}}$, where $\lambda \in [0, ..., 1]$,

$$T_{\mathrm{f},1} = G_\mathrm{f}\dot{q}_{\mathrm{f},3,\mathrm{nom}}\lambda \tag{8}$$

where we note again that $\dot{q}_{\mathrm{f},3,\mathrm{nom}}$ is constant under the assumptions stated above. We use PI control

$$u(t) = K_{\mathrm{P}} e(t) + K_{\mathrm{I}} \int_0^t e(\tau) d\tau, \tag{9}$$

where $u(t) = \lambda(t)$ is the controller output and $e(t) = T_{\mathrm{f,3,nom}} - T_{\mathrm{f,3}}$ is the control error. The parameters $K_{\mathrm{P}}$ and $K_{\mathrm{I}}$ are determined such that the closed-loop shows fastest response without overshoot using the root locus method. The solar irradiation and the inlet temperature at the collector field are assumed to act as unknown disturbances on the system. A linear description of the molten heat to HTF exchanger can be obtained from linearizing (3). It reads

$$T_{\mathrm{f,2,b}} = G_{\mathrm{f,f}}(1-\lambda)\dot{q}_{\mathrm{f,3,nom}} + G_{\mathrm{f,s}}\dot{q}_{\mathrm{s}}, \tag{10}$$

where $\dot{q}_{\mathrm{s}}$ is the molten salt flow rate and $(1-\lambda)\dot{q}_{\mathrm{f,3,nom}}$ is the flow from $L_1(\lambda)$ (see Fig. 4(a)). The transfer functions $G_{\mathrm{f,f}}$ and $G_{\mathrm{f,s}}$ are given by

$$G_{\mathrm{f,f}} = \frac{-3.32s - 0.43}{s^2 + 13.47s + 0.48} \quad \text{and} \quad G_{\mathrm{f,s}} = \frac{0.42}{s^2 + 13.47s + 0.48} \cdot 10^{-2},$$

respectively. Note that $(1-\lambda)\dot{q}_{\mathrm{f,3,nom}}$ acts as a disturbance on this system. Since $\lambda$ is given and $\dot{q}_{\mathrm{f,3,nom}}$ is assumed to be constant, this disturbance is known and can be compensated by setting

$$\dot{q}_{\mathrm{s}} = -\frac{G_{\mathrm{f,f}}}{G_{\mathrm{f,s}}}(1-\lambda)\dot{q}_{\mathrm{f,3,nom}} + \dot{\tilde{q}}_{\mathrm{s}},$$

and considering $\dot{\tilde{q}}_{\mathrm{s}}$ to be the input. Unfortunately, the compensator transfer function $\frac{G_{\mathrm{f,f}}}{G_{\mathrm{f,s}}}$ is not realizable. This problem can be overcome by setting

$$\dot{q}_{\mathrm{s}} \approx -\frac{G_{\mathrm{f,f}}}{G_{\mathrm{f,s}}}\frac{1}{T_r s + 1}(1-\lambda)\dot{q}_{\mathrm{f,3,nom}} + \dot{\tilde{q}}_{\mathrm{s}}, \tag{11}$$

which yields

$$T_{\mathrm{f,2,b}} = G_{\mathrm{f,f}}\left(1 - \frac{1}{T_r s + 1}\right)(1-\lambda)\dot{q}_{\mathrm{f,3,nom}} + G_{\mathrm{f,s}}\dot{q}_{\mathrm{s}}.$$

The term $(1 - \frac{1}{T_r s+1})$ describes a high-pass filter, which damps signals with frequencies $\omega < \frac{1}{T_r}$. Assuming that the solar irradiation and thus the HTF flow rate changes slowly, $1 - \frac{1}{T_r s+1} \approx 0$ holds for $T_r$ sufficiently small and the transfer characteristics simplifies to $T_{\mathrm{f,2,b}} = G_{\mathrm{f,s}}\dot{\tilde{q}}_{\mathrm{s}}$. We use a PI controller, which has been tuned with the root-locus method, to regulate $T_{\mathrm{f,2}}$ to $T_{\mathrm{f,2,nom}} = 674K$.

Note that choosing the valve as the controller input and using the disturbance compensation (11) decouples the multi-input multi-output system defined by the differential equations (8) and (10), which describe the solar field and the heat exchanger, respectively. Decoupling results in the two single-input single-output systems

$$\begin{aligned} T_{\mathrm{f,1}} &= G_{\mathrm{f}}\dot{q}_{\mathrm{f,3,nom}}\lambda, \\ T_{\mathrm{f,2,b}} &= G_{\mathrm{f,s}}\dot{\tilde{q}}_{\mathrm{s}}. \end{aligned} \tag{12}$$

*Daytime operation:* During daytime, more energy is collected in the solar field than necessary for nominal operation. The excess energy can be used to charge the molten salt heat storage. We use the three way valve $L_2(\mu)$ to split the HTF between the steam generator and the molten salt heat exchanger (see Fig. 4(b)). Since the flow rate to the steam generator, $\dot{q}_{\mathrm{f,3}}$, is assumed to be fixed, the parameter $\mu$ can be calculated from $\mu = \frac{\dot{q}_{\mathrm{f,3,nom}}}{\dot{q}_{\mathrm{f,1}}}$.

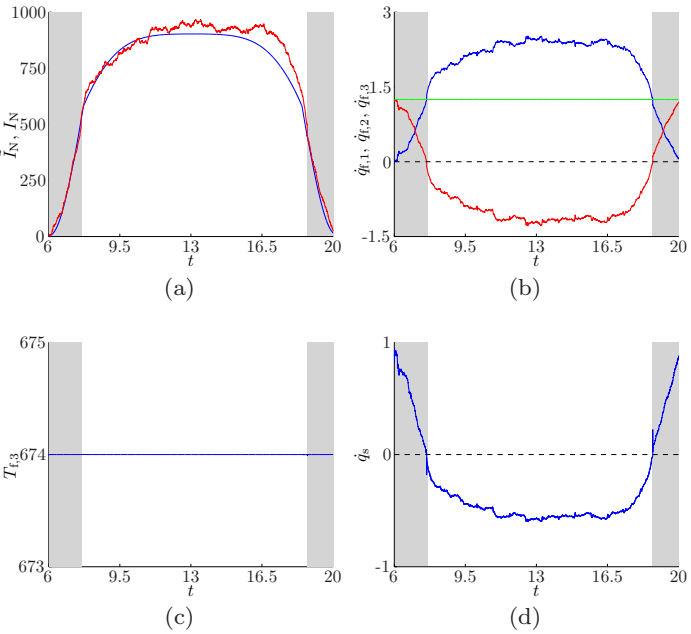


Fig. 5. Day-to-day collector data: (a) Solar irradiation $\tilde{I}_{\mathrm{N}}$ (blue) and the irradiation with random walk disturbance $\tilde{I}_{\mathrm{N}}$ (red) between 6AM and 8PM. Grey background indicates sunrise and sunset times, when the storage system is used as an additional energy source. White background indicates storage charging. (b) HTF flow rate through the collector field $\dot{q}_{\mathrm{f,1}}$ (blue), steam generator $\dot{q}_{\mathrm{f,3}}$ (green) and the salt to HTF heat exchanger $\dot{q}_{\mathrm{f,2}}$ (red). Opposite signs of $\dot{q}_{\mathrm{f,2}}$ indicate opposite flow directions; negative values corresponds to charging, positive values to storage discharging. (c) HTF temperature at the steam generator $T_{\mathrm{f,3}}$ is constant over the day-to-day cycle. (d) Molten salt flow rate through the molten salt to HTF heat exchanger $\dot{q}_{\mathrm{s}}$. Signs indicate flow direction.

Consider the linear model of the collector field again. Assuming that the inlet temperature and the solar irradiation are unknown disturbances,

$$T_{\mathrm{f,1}} = G_{\mathrm{f}}\dot{q}_{\mathrm{f,1}}, \tag{13}$$

where now the HTF flow rate $\dot{q}_{\mathrm{f,1}}$ is the controller input. By following the same steps as for (8) we find $\tilde{K}_I = \frac{K_I}{\dot{q}_{\mathrm{f,3,nom}}}$ and $\tilde{K}_P = \frac{K_P}{\dot{q}_{\mathrm{f,3,nom}}}$, where $K_I$ and $K_P$ are the parameters of the PI controller for (8).

The fraction of HTF that is not delivered to the steam generator is used to charge the molten salt storage. Linearizing (4) yields $T_{\mathrm{s,b}} = G_{\mathrm{s,f}}(1-\mu)\dot{q}_{\mathrm{f,1}} + G_{\mathrm{s,s}}\dot{q}_{\mathrm{s}}$, where $(1-\mu)\dot{q}_{\mathrm{f,1}}$ is a known disturbance, and the transfer functions read

$$G_{\mathrm{s,f}} = \frac{-13.62}{s^2 + 6.46s + 0.04} \cdot 10^{-2} \quad \text{and} \quad G_{\mathrm{s,s}} = \frac{3.65s + 23.48}{s^2 + 6.46s + 0.04}.$$

This disturbance can be compensated again using the compensator $\dot{q}_{\mathrm{s}} = -\frac{G_{\mathrm{s,f}}}{G_{\mathrm{s,s}}}(1-\mu)\dot{q}_{\mathrm{f,1}} + \dot{\tilde{q}}_{\mathrm{s}}$ with the artificial input $\dot{\tilde{q}}_{\mathrm{s}}$. In summary, this yields $T_{\mathrm{f,1}} = G_{\mathrm{f}}\dot{q}_{\mathrm{f,1}}$, $T_{\mathrm{s,b}} = G_{\mathrm{s,s}}\dot{\tilde{q}}_{\mathrm{s}}$. In contrast to (12), the salt output temperature is chosen as the second output.

### 2.2 Steam generation

Since the turbine is modeled as a multi-group turbine with pre- and reheater, and the thermal properties of water and steam are not assumed to be constant, this part of the power plant is a nonlinear multi-input multi-output system. For simplicity, we assume that (a) the ratio of the steam generator HTF flow rate to the reheater HTF flow rate is fixed, (b) the temperature of the cooling water is constant, (c) the pipes are ideal, and (d) a constant mass flow $\dot{m}_{\mathrm{V}}$ is withdrawn to preheat the feedwater.

We apply inlet pressure control to control this part of the plant. This type of controller stabilizes the pressure $p_1$ before the high pressure group of the turbine using the input valve $u_{\mathrm{V}}$ (see Fig. 3). The mass flow through the high pressure group and thus the thermal power output varies in this case. The linear input to output dynamics from input $u_{\mathrm{V}}$ to output $p_1$ can be found by linearizing the turbine, the pre- and reheater, and the steam generator at their nominal operation points and can be written as

$$p_1 = \tilde{G}_{\mathrm{SG}} u_{\mathrm{V}}. \tag{14}$$

Computing a reduced order approximation of (14) results in the transfer function $G_{\mathrm{SG}}$, which has four stable poles and two complex-conjugate zeros with negative real part and reads $G_{\mathrm{SG}} = \frac{1.44s^2 - 9.31s - 16.02}{s^4 + 25.56s^3 + 126.9s + 6.59} \cdot 10^7$. A standard PI controller has been used to compensate the slowest pole of $G_{SG}$, and the controller gain was chosen such that the resulting closed loop shows aperiodic behavior with the root locus method.

## 3. SIMULATION AND RESULTS

We simulate the power plant for an entire day to assess the performance of the proposed controllers. The nonlinear subsystems described in Sec. 1 are implemented in C, and an implementation of the IAPWS-IF97 formulas in C are used. The simulations are carried out using Matlab/Simulink. Before discussing simulation results, we summarize the calculation of the solar irradiation. The solar irradiation consists of two contributions, the direct and the diffuse irradiation. Since the power output of solar plants mainly depends on the direct irradiation, we neglect the diffuse component.There exist various methods for the estimation of the solar irradiation at ground level. We choose the European Solar Radiation Atlas (ESRA) clear-sky model. According to Rigollier et al. (2000) the direct solar irradiation is given by

$$I = I_0 \epsilon_0 \sin(\psi) e^{-0.8662 T_L m \delta}$$

where $I_0 = 1367 \frac{\mathrm{W}}{\mathrm{m}^2}$ is the solar constant, $\epsilon_0$ is a correction term, $\psi$ is the solar altitude angle, $T_L$ is the Linke turbidity factor, $m$ is the relative optical air mass and $\delta$ is the integral Rayleigh optical thickness. Both the relative optical air mass and the integral Rayleigh optical thickness depend on the altitude above sea level. We refer to Rigollier et al. (2000) and references therein for the calculation of $T_L$, $m$ and $\delta$.

The calculated solar irradiation $I$ holds for a surface normal to the inclination angle. In most plants, the collectors track the sun over the day to maximize the collected energy. In the plant considered here, however, the tracking is only uniaxial, which leads to an error that can be modeled by

$$\tilde{I}_{\mathrm{N}} = I \cos(\Theta).$$

The inclination angle $\Theta$ depends on the solar altitude angle and the location of the plant. It can be calculated from simple geometric considerations (Quaschning, 2011, p. 63 ff.).

We add a random walk to $\tilde{I}_N$ to model measurement errors. More precisely, the solar irradiation used for simulations in this paper is modeled by

$$I_{\mathrm{N}} = \tilde{I}_{\mathrm{N}} + \xi(t), \tag{15}$$

where $\xi(t) = \sum_{i=1}^{k} \tau_i(k\tilde{T})$, with a uniformly distributed random variable $\tau_i(k\tilde{T}) \in [-5, 5]$, where $\tilde{T} = 25\mathrm{s}$ is the sample time. The interval limits and the sample time have been chosen such that the effect of the disturbance is reasonable.

Steam generators or steam turbines are often tapped to draw steam for other purposes than electrical energy generation, for example, for simple heating purposes. Since disturbances of this type are common, we assume the steam generator is tapped and steam is extracted at a time-varying mass flow rate $\dot{m}_{\mathrm{D}}(t)$. Specifically, we assume $\dot{m}_{\mathrm{D}}(t)$ to be the periodic function

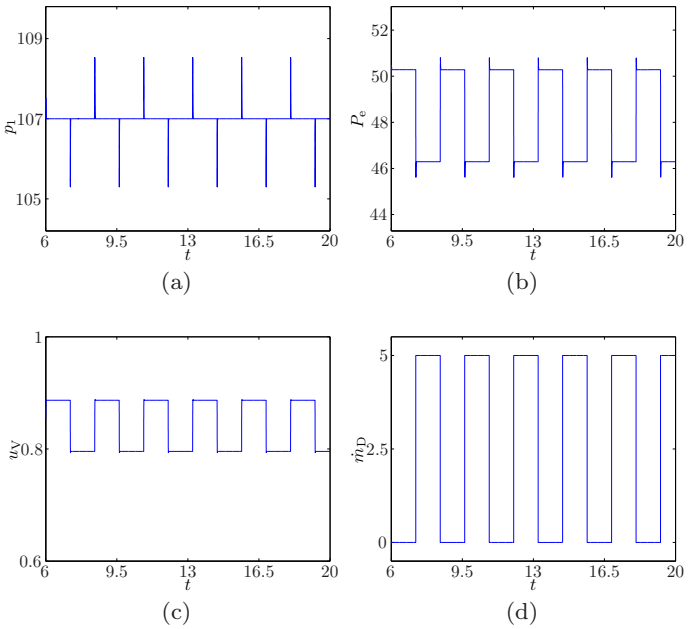


Fig. 6. Results of the steam generation part for the simulated day-to-day cycle: (a) Inlet pressure to the high pressure group of the turbine is stabilized by the controller. (b) Generated power of the solar plant. If the extracted mass flow $\dot{m}_{\mathrm{D}}$ increases, the mass flow through the turbine decreases, consequently the generated power decreases. (c) The inlet valve at the turbine is used as the control input: if the mass flow through the turbine decreases, the pressure at the turbine decreases. The controller closes the valve to regulate the pressure back to its nominal level. (d) Extracted mass flow $\dot{m}_{\mathrm{D}}$, see (16).

$$\dot{m}_{\mathrm{D}} = \begin{cases} 5\,\mathrm{Kg\,s^{-1}} & 0 \le t - \left\lfloor \frac{t}{T} \right\rfloor T < \frac{T}{2} \\ 0\,\mathrm{Kg\,s^{-1}} & \text{else} \end{cases}, \qquad (16)$$

with period $T = 9000$s.

Simulation results for the controlled collector field are shown in Fig. 5. Figure 5(a) shows the calculated solar irradiation as well as the disturbed signal (15). The solar irradiation increases, and reaches a maximum around noon. As the irradiation increases, more and more HTF is routed through the collector field by the controller. During this period, the molten salt is used as a secondary energy source (Figs. 5(a,b)). When the HTF flow rate reaches $\dot{q}_{\mathrm{f,3,nom}}$, more heat is collected in the solar field than necessary to run the plant. The HTF flow rate through the collector field increases further, and the storage system is charged with the additional heat (sign of the molten salt flow rate indicates charging). When the solar irradiation drops below the nominal level $\dot{q}_{\mathrm{f,3,nom}}$, the storage is used as an additional energy source again to run the plant. Obviously, the temperature $T_{\mathrm{f,3}}$ and the flow rate through the steam generator $\dot{q}_{\mathrm{f,3}}$ are constant over the entire day-to-day cycle (Figs. 5(b,c)), which shows that the presented control strategy is able to stabilize the collector field despite the imposed disturbances. Fig. 5(d) shows the molten salt flow rate $\dot{q}_s$

Simulation results for the steam part are shown in Fig. 6. The inlet pressure to the high pressure group is shown in Fig. 6(a). Steam extraction according to (16) leads to a significant disturbance, but the controller is able to stabilize the pressure at 107bar. Not surprisingly, the generated power decreases if the mass flow through the turbine decreases (see Fig. 6(b)). Figure 6(c) shows the normalized valve position. Obviously, to increase the pressure in front of the turbine group after $\dot{m}_{\mathrm{D}}$ increases, the valve closes. Finally, the extracted mass flow rate $\dot{m}_{\mathrm{D}}$ is shown in Fig. 6(d).

## 4. SUMMARY AND OUTLOOK

We presented a plant-wide control strategy for a solar power plant with molten salt storage system. The strategy, which uses the three way valves in the thermal oil cycle as additional control inputs, has been shown to stabilize the inlet temperature and HTF flow rate at the steam generator during a day-to-day cycle with disturbances. Inlet pressure control was implemented to control the power generation block of the power plant. Our simulations show that the controller is able to regulate the inlet pressure to the turbine in the presence of disturbances.

Several extensions of the presented work can be outlined as follows. We used linear controllers that decouple the nonlinear multi-input multi-output system in Sec. 2.1. The linear models used to derive the controllers are only valid at the steady state of linearization. The controller performance may decrease if the plant is not operated under nominal conditions and the disturbance compensation may not be able to decouple the multi-input multi-output system. Moreover, some assumptions applied to the steam generation cycle can be dropped. For example, we assumed a fixed ratio of the steam generator and reheater HTF flow rates. This ratio can be considered to be an additional controller input. Finally, further research should address set point tracking for the inlet temperature and HTF flow rate at the steam generator for use in start-up and shut-down procedures of the power plant and the power cycle.

## Appendix A. THERMAL PROPERTIES OF FLUIDS

The density and heat capacity of a typical thermal oil can be modeled as

$$\rho_{\mathrm{f}} = 1071.0 - 0.6306(T_{\mathrm{f}} - 273.15) - 0.0007646(T_{\mathrm{f}} - 273.15)^2,$$
$$c_{\mathrm{f}} = 1510.8 + 2.254(T_{\mathrm{f}} - 273.15) + 0.00062631(T_{\mathrm{f}} - 273.15)^2,$$

respectively. For the density and heat capacity of the molten salt we assume

$$\rho_{\mathrm{s}} = 2265.38 - 0.64T_{\mathrm{s}},$$
$$c_{\mathrm{s}} = 1400.48 + 0.17T_{\mathrm{s}},$$

respectively. Thermal properties of water and steam are implemented based on the International Association for the Properties of Water and Steam (IAPWS-IF97) (Wagner and Kretzschmar, 1997).

## REFERENCES

Alduchov, O.A. and Eskridge, R.E. (1996). Improved Magnus form approximation of saturation vapor pressure. *Journal of Applied Meteorology and Climatology*, 35, 601–609.

Camacho, E.F., Berenguel, M., Valenzuela, L., and Rubio, F.R. (1997). *Advanced Control of Solar Plants*. Springer.

Camacho, E.F., Rubio, F.R., Alvarado, I., and Limon, D. (2010). Control of solar power systems: a survey. In *Proceedings of the 9th International Symposium on Dynamics and Control of Process Systems*, 817 – 822.

Camacho, E.F., Rubio, F.R., Berenguel, M., and Valenzuela, L. (2007a). A survey on control schemes for distributed solar collector fields Part I: Modeling and basic control approaches. *Solar Energy*, 81, 1240–1251.

Camacho, E.F., Rubio, F.R., Berenguel, M., and Valenzuela, L. (2007b). A survey on control schemes for distributed solar collector fields Part II: Advanced Control Approaches. *Solar Energy*, 81, 1252–1272.

Chapman, S.J. (2012). *Electric Machinery Fundamentals*. McGraw Hill.

Grote, W. (2009). *A contribution to model based control of extraction steam turbines (In German)*. Ph.D. thesis, Ruhr-Universität Bochum.

Gülich, J.F. (2010). *Centrifugal Pumps*. Springer.

Incropera, F.P., DeWitt, D.P., Bergman, T.L., and Lavine, A.S. (2007). *Fundamentals of Heat and Mass Transfer*. Wiley & Sons, 6th edition.

Leonow, S. and Mönnigmann, M. (2013). Soft sensor based dynamic flow rate estimation in low speed radial pumps. In *Proceedings of the European Control Conference 2013*, 778–783.

Pacheco, J.E., Showalter, S.K., and Kolb, W.J. (2001). Development of a molten-salt thermocline thermal storage system for parabolic trough plants. In *Proceedings of the Solar Forum 2001*.

Powell, K.M. and Edgar, T.F. (2011). Control of a large-scale solar thermal energy storage system. In *Proceedings of the 2011 American Control Conference*, 1536–1541.

Quaschning, V. (2011). *Regenerative Energiesysteme: Technologie – Berechnung – Simulation*. Carl Hanser Verlag, 7th edition.

Rigollier, C., Bauer, O., and Wald, L. (2000). On the clear sky model of the ESRA – European Solar Radiation Atlas – with respect to the heliosat method. *Solar Energy*, 68, 33–48.

Sonntag, R.E. and Van Wylen, G.J. (1971). *Introduction to Thermodynamics: Classical and Statistical*. John Wiley & Sons, Inc.

Wagner, W. and Kretzschmar, H.J. (1997). *International Steam Tables: Properties of Water and Steam based on the Industrial Formulation IAPWS-IF97*. Springer, 2nd edition.